Progress In Electromagnetics Research C, Vol. 119, 245–254, 2022

High-Gain Reflectarray with Compact Aperture Size and a Low Profile Using an Active-Integrated Feeding Antenna

Yen-Sheng Chen* and Yu-Hong Wu

Abstract—In this paper, we present a gain-enhancement technique for reflectarray applications with compact aperture size and a low profile. To increase antenna gain, reflectarrays are constructed as an electrically large aperture, and the feed is required to be of high directivity, which is accompanied by a longer focal length. This increases the dimensions in two aspects, including the physical aperture size and the profile of the overall structure. To obtain high gain with compact dimensions, we develop a reflectarray that uses an active-integrated feeding antenna. This feeding antenna is connected to a microwave power amplifier, which enhances the gain without reducing the half-power beam widths (HPBWs) of the patterns. Accordingly, the feed can be arranged with a shorter focal length, whereas the spillover efficiency is still high. Moreover, the power amplifier contributes additional gain of 20.6 dB, and thus the proposed structure can achieve realized gain as high as 44.5 dB with dimensions of 9.2×6.7 square wavelengths. Such a high-gain and compact antenna is particularly suitable for satellite applications.

1. INTRODUCTION

For gain-enhancement purposes, an antenna can accommodate with a reflectarray and a transmitarray. These structures prevent the fabrication complexity in conventional reflectors or lens, manufacturing the electromagnetic surface based on printed circuit board (PCB) technology. Previous studies have presented several reflectarray designs [1–6]. By arranging various unit cells following the requirement of in-phase radiation, the reflected waves create constructive interference, which increases the gain of the antenna.

In numerous scenarios, gain enhancement is the design goal of reflectarray. Previous studies have performed two schemes to improve the antenna gain. First, a straightforward method is to increase the aperture dimensions [7–10]. The dimensions of the reflectarray are 59.6×59.6 [7], 20.0×20.0 [8], 18.8×18.8 [9], and 15.2×15.2 [10] square wavelengths, respectively, whereas the gains are 42.0 dBi, 15.4 dBi, 32.8 dBi, and 28.7 dBi. However, the design space of the reflectarray is usually confined in a finite area. The gain enhancement cannot be obtained without the tradeoff of increased aperture size. The second method is to use a highly directive feed with narrow half-power beam widths (HPBWs) [11–13]. Because the gain of the feed is already high, the resultant gain of the reflectarray antenna can be further improved. The feeds are implemented as a patch array [11], a slot array [12], and a lens antenna [13], respectively, and the gains are 14.7 dBi, 10.0 dBi, and 23.3 dBi. Also, a large number of studies employ a horn antenna as the feed, for the horn antenna usually generates higher gain. However, the patterns of these highly directive feeds depict narrow HPBWs, which further reduce illumination efficiency unless a longer focal length is used [14]. As a result, this type of reflectarrays usually presents a large height in profile. In summary, both methods enhance the gain at the cost of increased horizontal or vertical dimensions.

Received 12 March 2022, Accepted 8 April 2022, Scheduled 19 April 2022
* Corresponding author: Yen-Sheng Chen (yschen@ntut.edu.tw).
The authors are with the Department of Electronic Engineering, National Taipei University of Technology, Taipei, Taiwan.

Using an active-integrated antenna (AIA) as a feed can mitigate these limitations. While AIAs include oscillator type, mixer type, and amplifier type [15–17], the amplifier-type AIA cascades an amplifier with an antenna, increasing the overall gain by biasing the amplifier. This approach increases the gain significantly with little additional design space. Besides, it does not reduce the HPBWs of the antenna, whereas the gain can be improved significantly. This further means that the focal length does not need to be enlarged for addressing the illumination efficiency. Thus, this technique is promising for the requirement of directive and compact antennas.

In this paper, we propose a high-gain reflectarray antenna without sacrificing the dimensions of the structure. The feed of the reflectarray is developed into an amplifier-type AIA using a quasi-Yagi antenna, which illuminates the reflectarray to create in-phase radiation. As the quasi-Yagi antenna depicts broad HPBWs, a shorter focal length can be implemented without reducing the illumination efficiency. The proposed mechanism has been demonstrated in a transparent design [18]; nevertheless, that earlier design features insufficient aperture efficiency, whereas this study validates the concept using a more general PCB technology with improved gain and aperture efficiency. Simulated and measured results will be provided to demonstrate the proposed antenna.

2. ACTIVE INTEGRATED FEEDING ANTENNA

Figure 1 shows the block diagram of the proposed reflectarray antenna. A power module is implemented to supply energy to the AIA and other on-board electronics. As a proof of concept, the amplifier-type AIA employs a low noise amplifier (LNA) HMC963LC4, from Analog Devices, Taiwan. By biasing a voltage of 3.5 V, the input current of the amplifier is 45 mA. The amplifier is cascaded with a quasi-Yagi antenna [18], whose geometry is demonstrated in Fig. 2. In this prototype, the quasi-Yagi antenna is designed at 25.0 GHz. This AIA functions as the feed of a reflectarray, creating incident waves from a normal direction. Although normal incidence may block the reflected waves, this effect is mitigated due to the end-fire pattern of the quasi-Yagi antenna.

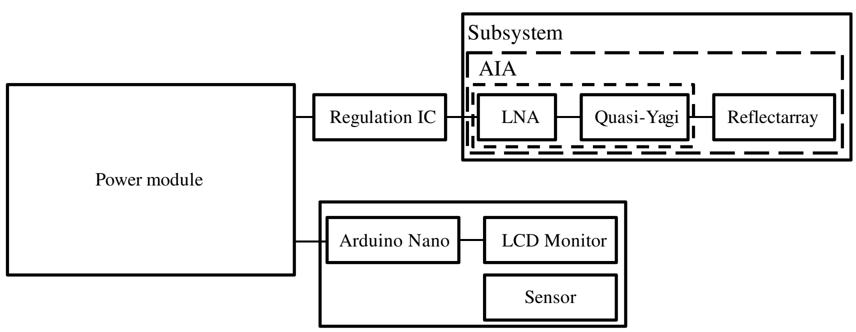

Figure 1. The block diagram of the proposed antenna.

The quasi-Yagi antenna is fabricated on a RO4350B substrate (relative permittivity $\varepsilon_r = 3.48$ and loss tangent $\tan\delta = 0.004$). Fig. 3 depicts the current distributions of the quasi-Yagi antenna. For the driven element, standard dipole-wise currents are observed. The directors are coupled with strong currents, indicating that they facilitate beam directing. As a result, the peak gain of the quasi-Yagi antenna alone is shown in Fig. 4. At 25.0 GHz, the gain is 7.6 dBi, whereas the HPBWs of the E-plane and H-plane are 55.5° and 93.0°, respectively. In comparison with horn antennas or earlier highly directive feeds [11–13], the beam area of the quasi-Yagi antenna is relatively large, and the gain is not significantly high. Nevertheless, due to the broad HPBWs, this antenna can be arranged with a short focal length featuring low profile, which is what the highly directive feeds cannot offer.

The circuit of the power module is shown in Fig. 5. As the maximum input voltage of the LNA is 3.5 V, the power module is connected to a regulation integrated circuit (IC) to limit the biasing voltage.

The design of the amplifier network is a multi-objective problem, including a minimized reflection coefficient, a maximized transmission coefficient, and unconditional stability illustrated by Rollet's K-

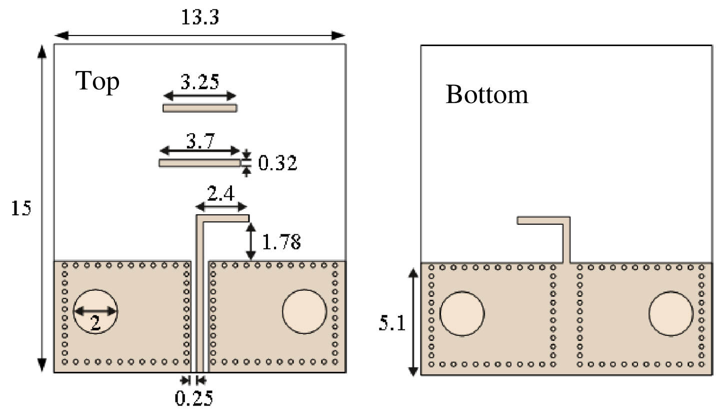

Figure 2. The geometry of the quasi-Yagi antenna (unit: mm).

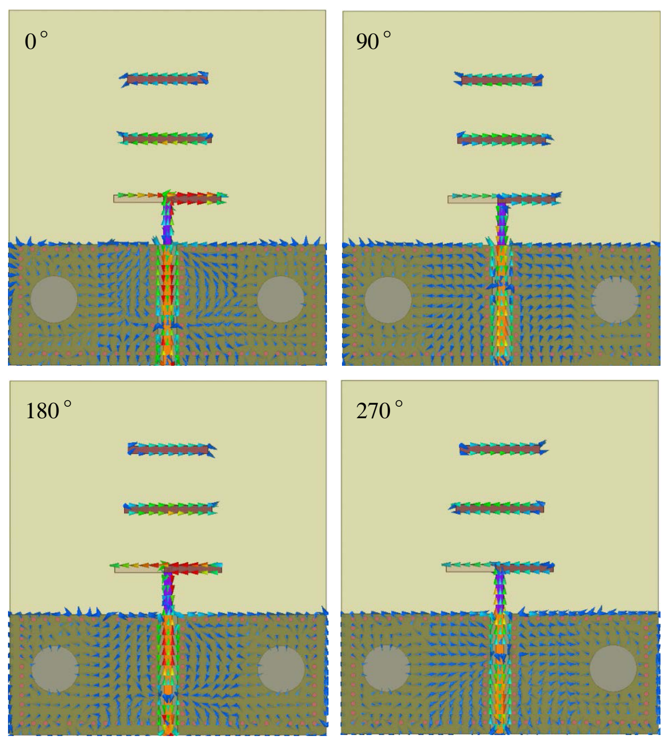

Figure 3. Simulated current distributions of the quasi-Yagi antenna at 25.0 GHz.

factor [19]:

$$K = \frac{1 - |S_{11}|^2 - |S_{22}|^2 + |\Delta|^2}{2\,|S_{12}|\,|S_{21}|} \tag{1}$$

where S_{11}, S_{12}, S_{21}, and S_{22} are the two-port scattering parameters of the amplifier, and Δ is the determinant of the matrix. A stable amplifier network should show K greater than 1. With the help of ADS optimization, the two-port power gain is shown in Fig. 6. At 25.0 GHz, the simulated and measured two-port transmission coefficients are 21.5 dB and 20.6 dB, respectively, whereas the reflection coefficients are below -10 dB. The corresponding K factor is 3.30, confirming that the LNA offers high transmission coefficients and stable performance.

Finally, the power module, LNA, and the quasi-Yagi antenna are integrated to test the gain of

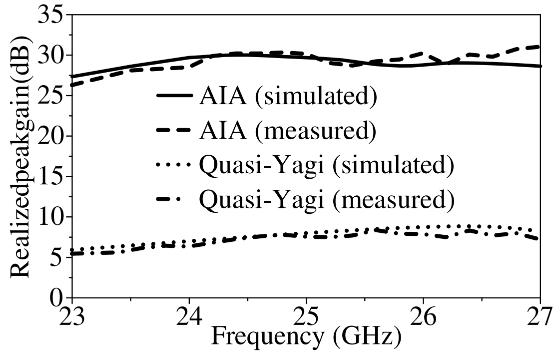

Figure 4. Comparison of the realized peak gain for the original quasi-Yagi antenna and the AIA.

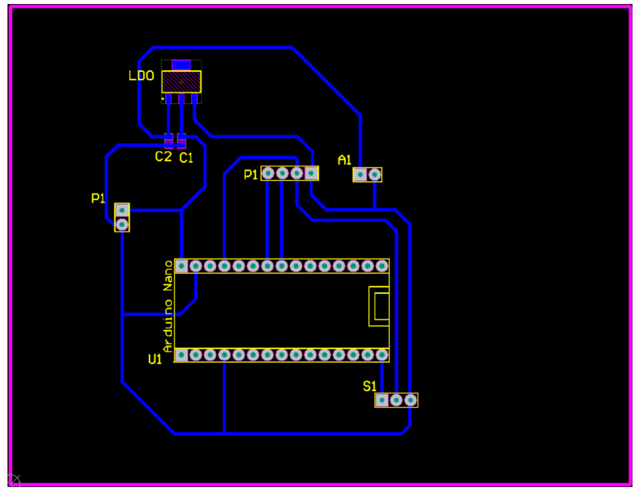

Figure 5. Circuit of power module for biasing the AIA.

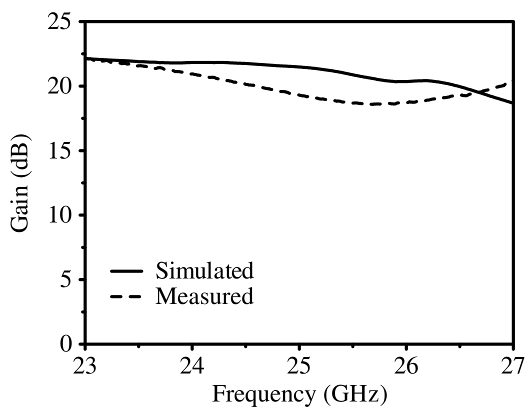

Figure 6. Gain spectrum of the LNA HMC963LC4.

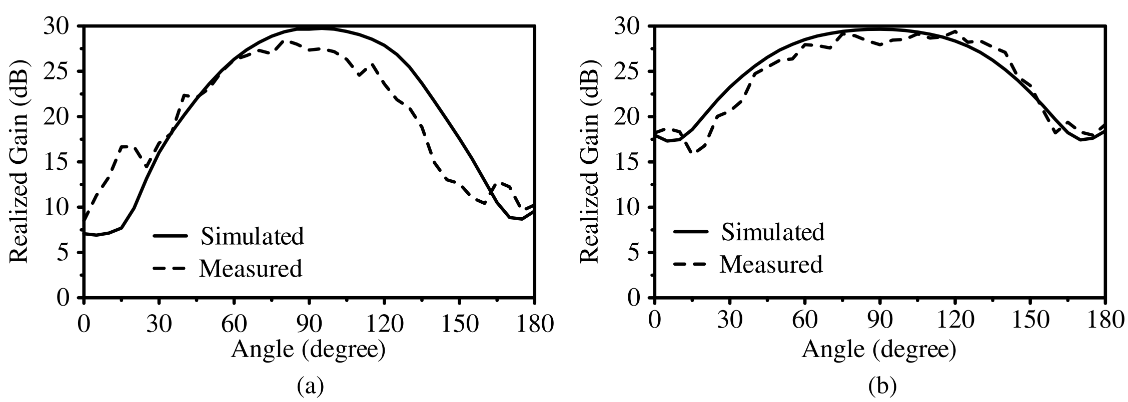

Figure 7. Gain pattern of the feeding AIA. (a) *E*-plane. (b) *H*-plane.

the feed. Such an AIA demonstrates desirable far-field performance. The realized gain is also depicted in Fig. 4, which indicates that the gain is improved as 30 dB. Fig. 7 demonstrates the patterns. In comparison with the original patterns of the quasi-Yagi antenna, the HPBWs are identical, thereby preserving the advantage of a short focal length. This suggests that the proposed technique can increase the gain of the antenna without reducing the beam area, so a low-profile structure can be achieved as compared to the use of a feeding horn.

3. REFLECTARRAY

Figure 8 presents the dimensions of the reflectarray. It is fabricated on a 0.813-mm-thick RO4003C substrate ($\varepsilon_r = 3.38$ and $\tan\delta = 0.003$). The dimensions are $110.0 \times 80.0\,\text{mm}^2$, where 25×19 unit cells are constructed. The unit cell employs rectangular patches. At 25.0 GHz, the tunable phase range is 296°, and the loss is 0.14 dB. In general, the tunable phase range of the unit cell is required to be 360°, whereas the result is insufficient. However, in comparison with other potential topologies, the rectangular patch shows the lowest loss, which is important for the gain-enhancement purpose. We remove the elements that cannot follow the phase requirement, generating the reflectarray using the ratio of the focal length to the maximum dimension that is 0.7 to 1. Such a focal length is particularly short for a feed illustrating gain as high as 30 dB. Fig. 9 demonstrates a photograph of the resultant reflectarray.

When the proposed reflectarray is fed by the quasi-Yagi antenna, the reflection coefficients are shown in Fig. 10. At 25.0 GHz, the simulated and measured reflection coefficients are −13.2 dB and

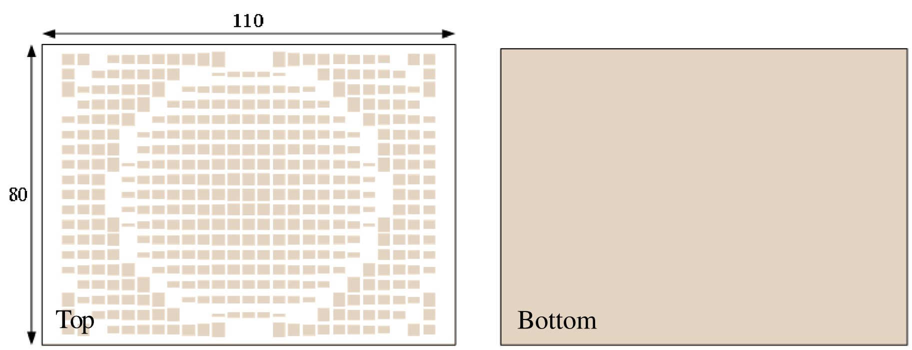

Figure 8. Dimensions of the reflectarray (unit: mm).

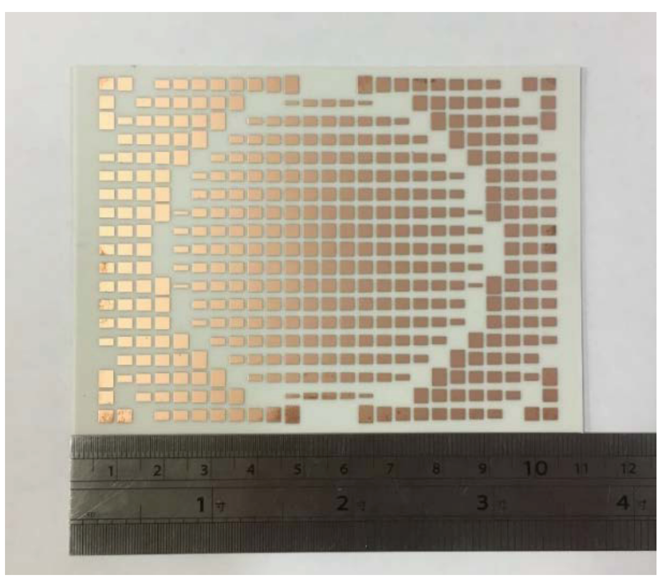

Figure 9. Photograph of the reflectarray.

$-12.1\,\text{dB}$. Good impedance matching is obtained. Fig. 11 is the peak gain of the reflectarray antenna. The simulated and measured gains at 25.0 GHz are 24.7 dBi and 22.5 dBi, respectively. Fig. 12 provides the antenna efficiency. Although the measured results are lower than the simulated ones, in general, the antenna efficiency is greater than 70%. Fig. 13 is the pattern of the reflectarray antenna. The HPBWs of the E-plane and H-plane are only 9°. Thus, the reflectarray enables highly directive radiation.

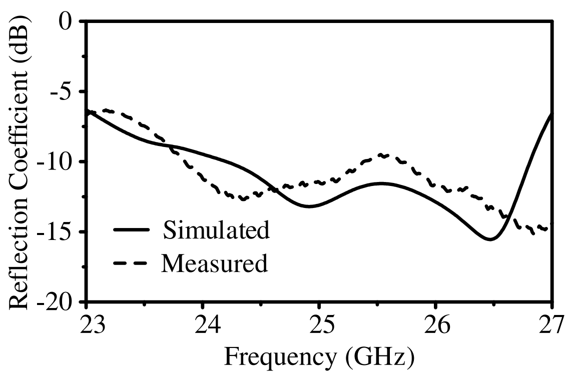

Figure 10. Reflection coefficients of the reflectarray fed by the quasi-Yagi antenna.

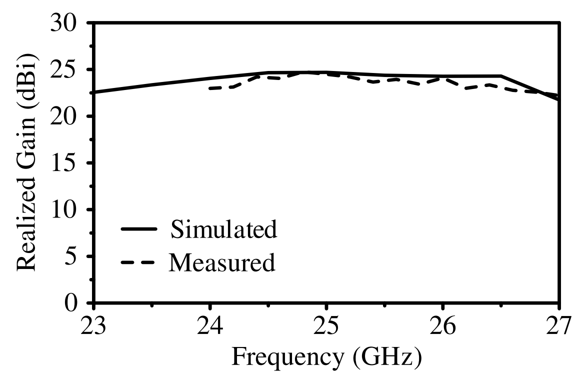

Figure 11. Gain spectrum of the reflectarray fed by the quasi-Yagi antenna.

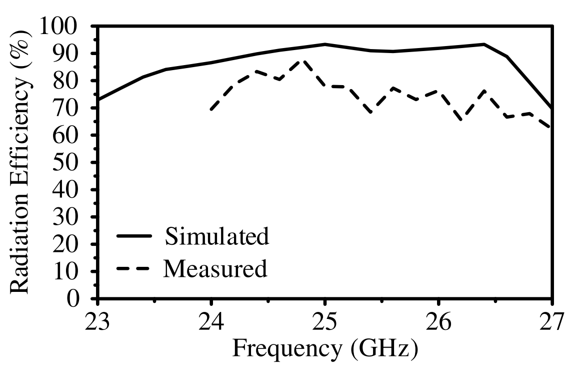

Figure 12. Antenna efficiency of the reflectarray fed by the quasi-Yagi antenna.

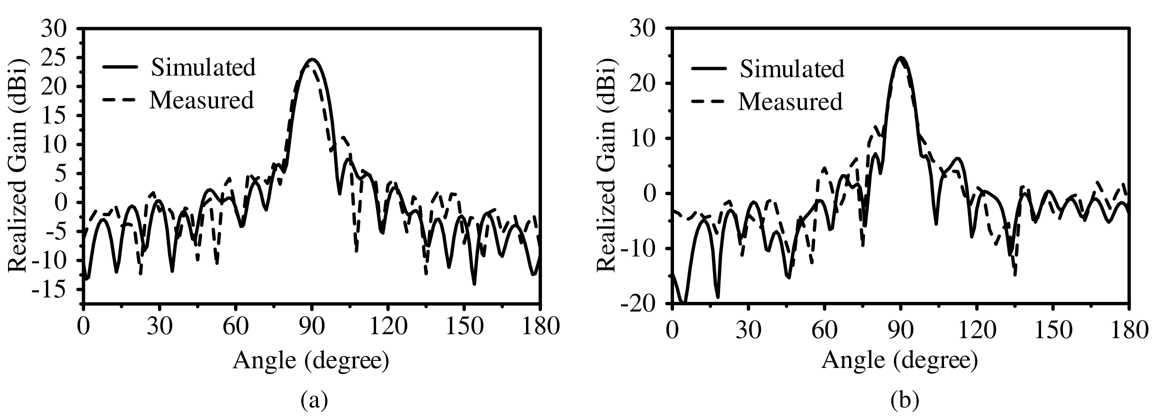

Figure 13. Gain pattern of the reflectarray fed by the quasi-Yagi antenna. (a) E-plane. (b) H-plane.

4. RESULTS

Finally, the proposed antenna is integrated, and the feed of the reflectarray is replaced by the AIA. A photograph of the overall structure is shown in Fig. 14. We bias the amplifier through the power module, whose location is inside the box made of three-dimensional (3D) printing. The antenna fixture is also manufactured using 3D printing, providing accurate positioning for the reflectarray. However, when testing the far-field performance, we remove the 3D-printing fixture and use Styrofoam board as the fixture. Fig. 15 shows a photograph of the far-field measurement.

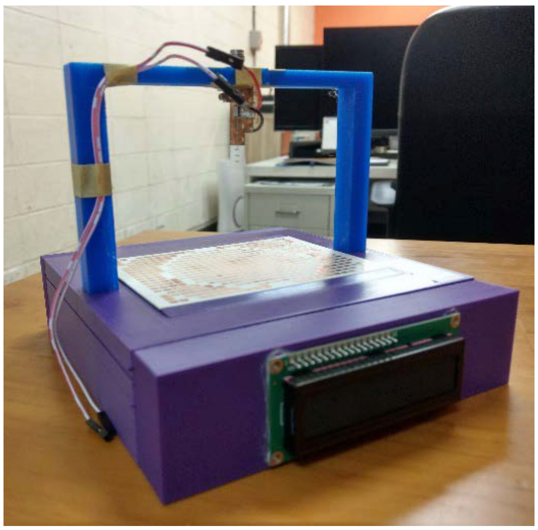

Figure 14. Photograph of the final antenna structure.

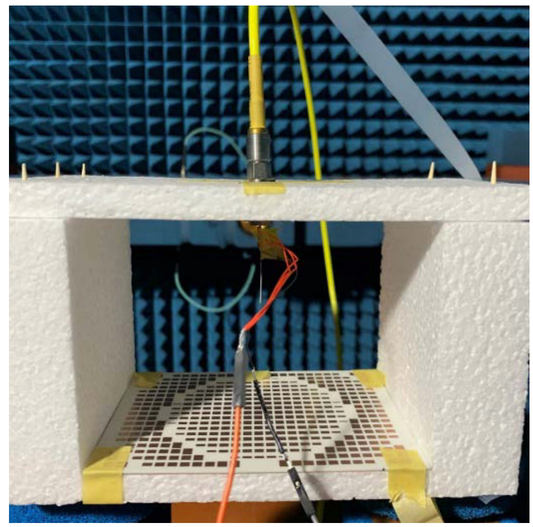

Figure 15. Far-field measurement of the proposed antenna.

Figure 16 is the simulated and measured impedance matching of the proposed antenna. The measured results show a frequency shift due to the loading effect of the mixture and other electronics. However, at the designed frequency, the reflection coefficient is still below -10 dB. The overall gain is shown in Fig. 17. The simulated and measured gains at 25.0 GHz are 46.0 dB and 44.5 dB, respectively. Considering that the design space of the reflectarray is only 9.2×6.7 square wavelengths, the obtaining measured gain of 44.5 dB is highly significant for a reflectarray application. Please note that the gain evaluation is not obtained by the comparison of a 3D pattern with that of an isotropic source. This feature can be illustrated by the unit of gain, which is dB, instead of dBi in the conventional case.

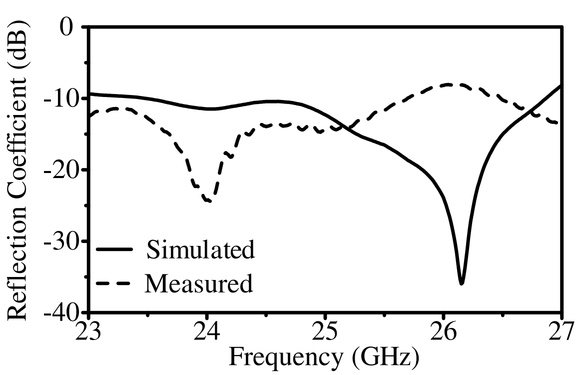

Figure 16. Reflection coefficients of the proposed antenna.

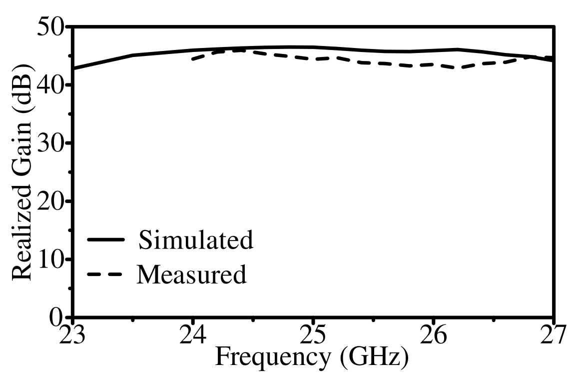

Figure 17. Gain spectrum of the proposed antenna.

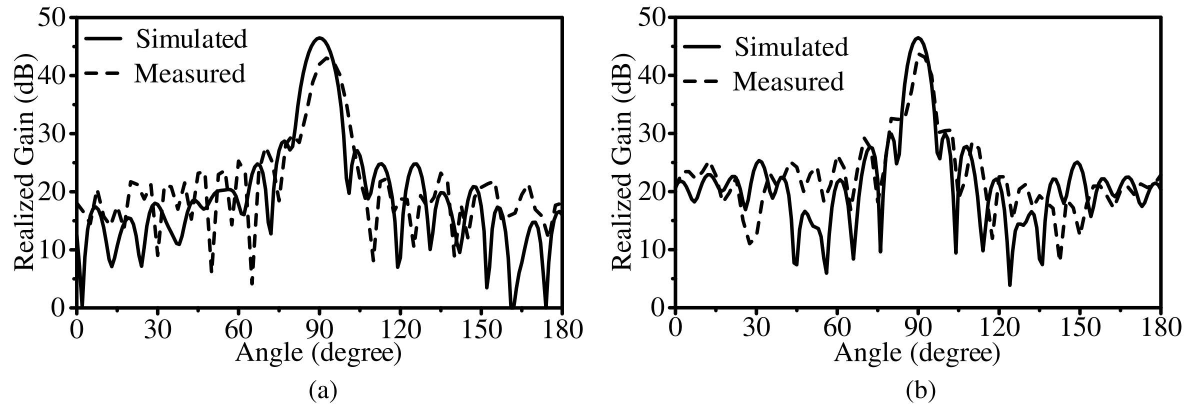

Figure 18. Gain pattern of the proposed antenna. (a) E-plane. (b) H-plane.

Due to the additional gain of the power amplifier, the maximum gain of the proposed reflectarray antenna is higher than the peak directivity evaluated from the 3D pattern. Thus, the conventional definition of radiation efficiency is not applicable in the amplifier-type AIA. Fig. 18 shows the simulated and measured patterns. The HPBWs are similar to the results shown in Fig. 13, whereas the gain is improved due to the AIA feed.

Moreover, the gain and aperture efficiency obtained in this study are significantly higher than the previous results [18]. Such an AIA feed integrated with a transparent reflectarray has led to measured peak gain of 41.3 dB and aperture efficiency of 23.3%. In this study, the validity of the proposed technique is obtained using more general PCB fabrication, and the results are improved by designing the reflectarray with greater aperture efficiency of 47.2%. Thus, with the same dimensions, the measured overall gain is as high as 44.5 dB.

Finally, the results achieved by the proposed technique are compared with earlier studies concerning the gain enhancement of reflectarrays. Table 1 depicts the dimensions of the reflectarrays and the realized peak gain. In comparison with the reflectarrays that employ large aperture size greater than 15.2×15.2 square wavelengths [7–10], the gain obtained using the AIA feed is significantly higher. The aperture size has to be 59.6×59.6 square wavelengths to attain peak gain of 42.0 dBi; in contrast, the proposed technique offers an even higher gain (44.5 dB) with dimensions of only 9.2×6.7 square wavelengths. This further indicates significant miniaturization provided by the proposed technique. In addition, for the earlier structures using a highly directive feed, such as a patch array [11], a slot array [12], and a lens antenna [13], the gain enhancement is not as strong as the proposed technique. While these studies implement smaller aperture size (such as 8.6×7.8 square wavelengths in [13]), the

Table 1. Realized peak gain and dimensions of the related studies.

Number	Technique	Dimensions ($\lambda \times \lambda$)	Measured peak gain
[7]	Large aperture size	59.6×59.6	42.0 dBi
[8]	Large aperture size	20.0×20.0	15.4 dBi
[9]	Large aperture size	18.8×18.8	32.8 dBi
[10]	Large aperture size	15.2×15.2	28.7 dBi
[11]	Highly directive feed	3.3×3.3	14.7 dBi
[12]	Highly directive feed	1.8×1.8	10.0 dBi
[13]	Highly directive feed	8.6×7.8	23.3 dBi
[18]	AIA feed	9.2×6.7	41.3 dB
This study	AIA feed	9.2×6.7	44.5 dB

maximum gain is lower than the proposed design by more than 20 dB. Besides, these highly directive feeds are accompanied by a longer focal length, which increases the height in profile. In summary, the proposed technique is attractive to high-gain reflectarrays with the requirement of compact aperture size and a short focal length.

5. CONCLUSION

In this paper, a compact reflectarray that uses an AIA feed has been presented. The compact dimensions are achieved in both horizontal area and vertical focal length. Thanks to the amplifier-type AIA, the feed depicts high gain and endfire patterns with a large beam area, which are particularly suitable for illuminating reflectarrays. Although the design space of the reflectarray is only 9.2×6.7 square wavelengths, the simulated and measured gains are 46.0 dB and 44.5 dB, respectively. Moreover, in terms of a feed providing peak gain of 30 dB, the HPBWs of the E-plane and H-plane patterns are 55.5° and 93.0°, respectively, so the ratio of the focal length to the maximum dimension can be arranged as only 0.7 to 1. The distinct characteristics of the proposed antenna can facilitate satellite applications to achieve greater performance. Future work is encouraged to modify the polarization of the proposed design into circular polarization, which is pursued in satellite communications. Also, beam-switching characteristics can be integrated in the reflectarray, leading to a reconfigurable intelligent surface with high gain and compact size.

REFERENCES

1. Pozar, D. M., S. D. Targonski, and H. D. Syrigos, "Design of millimeter wave microstrip reflectarrays," *IEEE Trans. Antennas Propag.*, Vol. 45, No. 2, 287–296, Feb. 1997.
2. Encinar, J. A. and J. A. Zornoza, "Three-layer printed reflectarrays for contoured beam space applications," *IEEE Trans. Antennas Propag.*, Vol. 52, No. 5, 1138–1148, May 2004.
3. Encinar, J. A., et al., "Dual-polarization dual-coverage reflectarray for space applications," *IEEE Trans. Antennas Propag.*, Vol. 54, No. 10, 2828–2837, Oct. 2006.
4. Hum, S. V. and J. Perruisseau-Carrier, "Reconfigurable reflectarrays and array lenses for dynamic antenna beam control: A review," *IEEE Trans. Antennas Propag.*, Vol. 62, No. 1, 183–198, Jan. 2014.
5. Narayanasamy, K., G. N. A. Mohammed, K. Savarimuthu, R. Sivasamy, and M. Kanagasabai, "A comprehensive analysis on the state-of-the-art developments in reflectarray, transmitarray, and transmit-reflectarray antennas," *Int. J. RF Microw. Comput. Aid. Eng.*, Vol. 30, No. 9, 1–22, Sep. 2020.
6. Zebrowski, M., "Illumination and spillover efficiency calculations for rectangular reflectarray antennas," *High Freq. Des.*, Vol. 1, 28–38, Dec. 2012.
7. Chahat, N., R. E. Hodges, J. Sauder, M. Thomson, E. Peral, and Y. Rahmat-Samii, "CubeSat deployable Ka-band mesh reflector antenna development for earth science missions," *IEEE Trans. Antennas Propag.*, Vol. 64, No. 6, 2083–2093, Jun. 2016.
8. Vourch, C. J. and T. D. Drysdale, "V-band 'Bull's eye' antenna for cubesat applications," *IEEE Antennas Wireless Propag. Lett.*, Vol. 13, 1092–1095, Jun. 2014.
9. Babuscia, A., et al., "Inflatable antenna for CubeSat: A new spherical design for increased X-band gain," *Proc. IEEE Aerospace Conference*, 1–10, Big Sky, MT, USA, Mar. 2017.
10. Moharram, M. A. and A. A. Kishk, "A Ka-band optically transparent reflectarray design integrated with solar cells," *Proc. IEEE International Conference on Ubiquitous Wireless Broadband (ICUWB)*, 1–4, Montreal, Canada, Oct. 2015.
11. Qin, F., et al., "Wideband circularly polarized Fabry-Perot antenna [antenna applications corner]," *IEEE Antennas Propag. Mag.*, Vol. 57, No. 5, 127–135, Oct. 2015.
12. Padilla, J., G. Rosati, A. Ivanov, F. Bongard, S. Vaccaro, and J. Mosig, "Multi-functional miniaturized slot antenna system for small satellites," *Proc. Eur. Conf. Antennas Propag. (EuCAP 2011)*, 2170–2174, Rome, Italy, May 2011.

13. McNicholas, M., J. Deluna, R. Manno, and Y.-H. Shu, "Low cost Ka-band transmitter for CubeSat systems," *Proc. Topical Workshop Internet Space (TWIOS)*, 1–4, Phoenix, AZ, USA, Jan. 2017.
14. Dahri M. H., et al., "Aspects of efficiency enhancement in reflectarrays with analytical investigation and accurate measurement," *Electronics*, Vol. 9, No. 11, 1–26, Nov. 2020.
15. Hang, C. Y., W. R. Deal, Y. Qian, and T. Itoh, "Push-pull power amplifier integrated with microstrip leaky-wave antenna," *Electron. Lett.*, Vol. 35, No. 22, 1891–1893, Oct. 1999.
16. Robert, B., T. Razban, and A. Papiernik, "Compact amplifier integration in square patch antenna," *Electron. Lett.*, Vol. 28, No. 19, 1808–1810, Sep. 1992.
17. Dhar, S. K., O. Hammi, M. S. Sharawi, and F. M. Ghannouchi, "Power amplifier based integrated and miniaturized active antenna," *Proc. 9th European Conference on Antennas and Propagation (EuCAP)*, 1–4, Lisbon, Portugal, Apr. 2015.
18. Chen, Y.-S., Y.-H. Wu, and C.-C. Chung, "Solar-powered active integrated antennas backed by a transparent reflectarray for CubeSat applications," *IEEE Access*, Vol. 8, 137934–137946, 2020.
19. Pozar, D. M., *Microwave Engineering*, 3rd Edition, Wiley, New York, NY, USA, 2005.